AD-A136 218 POSSIBLE DETECTION OF THERMAL CYCLOTRON LINES FROM SMALL SOURCES WITHIN S..(U) TUFTS UNIV MEDFORD MA DEPT OF PHYSICS R F WILLSON JUL 83 AFOSR-TR-83-1138 1/1

UNCLASSIFIED AFOSR-83-0019 F/G 3/2 NL

END

DATE FILMED

1-84

DTIC

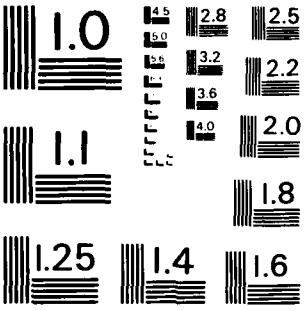

POSSIBLE DETECTION OF THERMAL CYCLOTRON LINES FROM SMALL SOURCES WITHIN SOLAR ACTIVE REGIONS

Robert F. Willson
Department of Physics
Tufts University
Medford, Massachusetts 02155

To appear in Solar Physics

SECURITY CLASSIFICATION OF THIS PAGE (When Data Entered)

REPORT DOCUMENTATION PAGE		READ INSTRUCTIONS BEFORE COMPLETING FORM
1. REPORT NUMBER AFOSR-TR- 83-1138	2. GOVT ACCESSION NO.	3. RECIPIENT'S CATALOG NUMBER
4. TITLE (and Subtitle) POSSIBLE DETECTION OF THERMAL CYCLOTRON LINES FROM SMALL SOURCES WITHIN SOLAR ACTIVE REGIONS		5. TYPE OF REPORT & PERIOD COVERED Interim 6. PERFORMING ORG. REPORT NUMBER
7. AUTHOR(s) Robert F. Willson		8. CONTRACT OR GRANT NUMBER(s) AFOSR-83-0019
9. PERFORMING ORGANIZATION NAME AND ADDRESS Tufts University Department of Physics Medford, MA 02155		10. PROGRAM ELEMENT, PROJECT, TASK AREA & WORK UNIT NUMBERS 61102F [redacted] 2311/A1
11. CONTROLLING OFFICE NAME AND ADDRESS AFOSR-NP Bolling AFB, Bldg. #410 Washington, D.C. 20332		12. REPORT DATE July 1983 13. NUMBER OF PAGES 23
14. MONITORING AGENCY NAME & ADDRESS(if different from Controlling Office)		15. SECURITY CLASS. (of this report) Unclassified 15a. DECLASSIFICATION DOWNGRADING SCHEDULE

16. DISTRIBUTION STATEMENT (of this Report)

Approved for public release; distribution unlimited

17. DISTRIBUTION STATEMENT (of the abstract entered in Block 20, if different from Report)

18. SUPPLEMENTARY NOTES

19. KEY WORDS (Continue on reverse side if necessary and identify by block number)

Sun: radio radiation - Sun: magnetic fields

20. ABSTRACT (Continue on reverse side if necessary and identify by block number)

Theoretical spectra of thermal cyclotron line emission from solar active regions are presented for two frequency bands available at the Very Large Array (VLA). VLA synthesis maps of three active regions at 1380, 1540 and 1705 MHz are then presented. The maps of two of these regions show significant changes in the brightness temperature within these narrow frequency ranges. We show that these changes may be attributed to thermal cyclotron line emission in small regions (θ = 10" to 30") where the magnetic

DD FORM 1 JAN 73 1473

Unclassified
SECURITY CLASSIFICATION OF THIS PAGE (When Data Entered)

field is relatively constant with H = 125-180 Gauss. An alternative interpretation, involving height-dependent variations in the physical conditions may also explain the changes in one of these regions. The potential to study coronal magnetic fields using VLA observations of cyclotron lines is also discussed.

ABSTRACT

Theoretical spectra of thermal cyclotron line emission from solar active regions are presented for two frequency bands available at the Very Large Array (VLA). VLA synthesis maps of three active regions at 1380, 1540 and 1705 MHz are then presented. The maps of two of these regions show significant changes in the brightness temperature within these narrow frequency ranges. We show that these changes may be attributed to thermal cyclotron line emission in small regions (θ = 10" to 30") where the magnetic field is relatively constant with H = 125-180 Gauss. An alternative interpretation, involving height-dependent variations in the physical conditions may also explain the changes in one of these regions. The potential to study coronal magnetic fields using VLA observations of cyclotron lines is also discussed.

1. INTRODUCTION

It was realized more than two decades ago that the cyclotron radiation (or gyroemission) of thermal electrons accelerated in solar magnetic fields may compete with the bremsstrahlung of thermal electrons accelerated in the electric fields of coronal ions (Stepanov 1959; Ginzburg and Zheleznyakov 1959). At the time, peculiarities in the frequency spectrum and polarization of solar active regions at radio wavelengths were interpreted in terms of the combined effects of cyclotron radiation and bremsstrahlung (Zheleznyakov 1962; Kakinuma and Swarup 1962). The observations used in support of this interpretation were, however, made with relatively small antennas whose large beamwidths could not resolve the individual sources within active regions. Interferometric observations at centimeter wavelengths indicated that beam dilution effects had, in fact, previously prevented the detection of small, intense sources which were very highly circularly polarized (Kundu 1959; Enome et al. 1969; Lang 1974). This high polarization could only be attributed to cyclotron radiation. Early observations of solar active regions with the Very Large Array (VLA) at 6 cm wavelength then revealed unusually hot ($\sim 10^6$ K) and highly circularly polarized (up to 95%) radiation above sunspots (Lang and Willson 1979; Kundu, Schmahl and Rao 1981). This radiation was attributed to the cyclotron radiation of coronal electrons trapped within the legs of magnetic dipoles whose feet are found in lower lying sunspots (Alissandrakis, Kundu and Lantos 1980; Lang, Willson and Gaizauskas 1983). In the meantime, observations at X-ray wavelengths had indicated that magnetic loops are the dominant structural features of the corona, but that the X-ray emission is most intense in the regions which lie above sunspots. The relatively weak X-ray radiation above sunspots implied low electron densities in these regions and this meant that bremsstrahlung could not account for the 6 cm emission

above sunspots (Pallavicini, Sakurai and Vaiana 1981). Additional opacity due to gyroresonant absorption was required to explain the high brightness temperatures at radio wavelengths. The presence of cyclotron radiation in the coronal atmosphere above sunspots was then confirmed by accurate polarization measurements at 6 cm wavelength using the Westerbork Synthesis Radio Telescope (WSRT) (Lang and Willson 1982). The observations indicated that highly polarized (up to 100%) horseshoe structures overlie sunspot penumbrae. These structures can only be explained by cyclotron radiation, and they had, in fact actually been predicted by the theory of gyroresonant absorption above individual sunspots (Gel'freikh and Lubyshev 1979).

The theory of cyclotron absorption indicates that observations at a given frequency, ν, refer to a narrow layer in the solar atmosphere at which $\nu = s\nu_H$, where $s = 2,3,4...$ is the harmonic, the gyrofrequency $\nu_H = 2.8 \times 10^6$ H Hz, and H is the magnetic field strength in Gauss. Because the magnetic field strength of dipolar loops decreases systematically with height above the solar photosphere, it was thought that the individual cyclotron lines would be superimposed to give a continuum spectrum, but that observations at longer wavelengths would refer to higher altitudes above the photosphere. Nevertheless, theoretical work predicted that individual cyclotron lines might be detected if the radiation was confined to a fixed altitude where the magnetic field is relatively constant. This might, for example, occur when neutral current sheets develop and subsequently rupture, thereby giving rise to solar bursts (Syrovatskii and Kuznetsov 1980; Kuznetsov and Syrovatskii 1981). The cyclotron radiation is able to escape only from a thin edge of the current sheet where the magnetic field is practically homogeneous. It was therefore imagined that thermal cyclotron lines might be detected during the temperature enhancements that occur before and during solar flares or bursts

(Zheleznyakov and Zlotnik 1980; Zheleznyakov and Tikhomorov 1980.) Zheleznyakov and Zlotnik (198) have pointed out that cyclotron lines might also be detected from quiescent active regions if the loop geometry allowed observations of relatively constant magnetic field. Kaverin et al. (1980) have, in fact, detected narrow band structures at centimeter wavelengths from several active regions. They suggested that these structures may be attributed to cyclotron line emission from small sources within these regions where the magnetic field is nearly uniform.

The optical depths, τ_{s_e} and τ_{s_o}, for the extraordinary and ordinary modes for an individual cyclotron line at harmonic s are given by (Zheleznyakov and Zlotnik 1980; Zheleznyakov 1970):

$$\tau_{s_{o,e}} = 3.93 \frac{\nu}{c} \left(\frac{\nu_p}{\nu} \right)^2 \frac{s^{2s}}{2^s s!} \beta_T^{2s-3} L_H F(\alpha) \exp(-z^2) \qquad (1)$$

where

$$F(\alpha) = (1 \pm \cos\alpha)^2 \frac{\sin\alpha^{2s-2}}{|\cos\alpha|}$$

and

$$z = \frac{\nu - s\nu_H}{\sqrt{2\nu\beta_T \cos\alpha}}$$

Here, the frequency $\nu = s\nu_H$, the gyrofrequency is $\nu_H = 2.8 \times 10^6$ H, the velocity of light is c, the plasma frequency $\nu_p = 8.9 \times 10^3 N_e^{1/2}$ for an electron density of N_e, the factor $\beta_T = V_{th}/c = 3.89 \times 10^5 T_e^{1/2}/c$ for an electron thermal velocity V_{th} and an electron temperature of T_e, and L_H is the scale length of the magnetic field. The function $F(\alpha)$ depends on the angle α, between the magnetic field and the line of sight and the + and - signs denote the extraordinary and ordinary modes of wave propagation. The Gaussian function $\exp(-z^2)$ describes a Doppler broadened line with a peak value of unity at $\nu = s\nu_H$ and a full width to half maximum of $\Delta\nu_D = 2.335\ \beta_T\nu$.

In addition to cyclotron emission, thermal bremsstrahlung can also contribute to the opacity above active regions. The optical depths τ_{B_e} and

τ_{B_o}, of the extraordinary and ordinary modes due to thermal bremsstrahlung are given by:

$$\tau_{B_e} = \frac{\tau_B}{[1 - \frac{\nu_H \cos\alpha}{\nu}]^2} \qquad (2)$$

$$\tau_{B_o} = \frac{\tau_B}{[1 + \frac{\nu_H}{\nu} \cos\alpha]^2}$$

where $\tau_B = \frac{9.78 \times 10^{-3} N_e^2 L}{\nu^2 T_e^{3/2}} \ln [4.7 \times 10^{10} T_e/\nu]$

is the classical expression for the bremsstrahlung optical depth in the absence of a magnetic field. The brightness temperatures $T_{B_{e,o}} = [1-\exp(-\tau_{e,o})]T_e$ where $\tau_{e,o} = \tau_{e,o} = \tau_{s_{e,o}} + \tau_{B_{e,o}}$. We have calculated the brightness temperature $T_B = (T_{B_e} + T_{B_o})/2$ and the degree of circular polarization $\rho_c = [T_{B_e} + T_{B_o}]/[T_{B_e} - T_{B_o}]$ as a function of frequency for the harmonics 2,3,4 and 5 and a number of different values of the magnetic field strength, temperature, density, scale length and angle. The results of our calculations for two frequency bands between 1000 and 2000 MHz and 4000-5000 MHz are shown in Figures 1 and 2. These frequency ranges were chosen because they are centered on two of the frequency bands available at the VLA. As illustrated in these figures, we obtain thermal cyclotron lines of half-width $\Delta\nu_D$ = 50-150 MHz, superimposed upon optically thin bremsstrahlung. Because τ_s depends strongly on the harmonic s, the cyclotron lines become optically thick at s = 2, 3, and 4 with flat tops and broad widths which refer to the lower, truncated parts of the Gaussian function $\exp(-z^2)$. Because $\Delta\nu_D/\nu$ is a constant, the lines between 4 and 5 GHz are about a factor of 3 wider than those between 1 and 2 GHz. Thus, under favorable conditions, observations of active regions at closely spaced frequencies may show jumps or more complicated variations in both the total intensity and circular polarization. In the next section, we describe observations of two active regions which, in fact, show such changes, and which may be attributed to thermal cyclotron line emission.

2. POSSIBLE DETECTION OF THERMAL CYCLOTRON LINES

It has been shown that VLA observations of quiescent active regions at centimeter wavelengths delineate the ubiquitous coronal loops that were previously detected at X-ray wavelengths (Kundu and Velusamy 1980; Lang, Willson and Rayrole 1982). The brightness temperatures of $T_B \approx 2 \times 10^6$ K suggested that the radio emission was due to the optically thick bremsstrahlung of a hot plasma trapped within the magnetic loops. Under this interpretation an electron density of $N_e \approx 5 \times 10^9$ cm^{-3} and a line of sight thickness of $L \approx 10^9$ cm are inferred. The classical expression for the bremsstrahlung optical depth, τ_B, (Eq.2) indicates that it is very close to unity at an observing frequency of $\nu \approx 1400$ MHz under these conditions. We therefore planned observations at three frequencies near 1400 MHz with the hope of detecting optically thin bremsstrahlung ($\tau_B < 1$). Because the observations at these frequencies refer to the upper parts of coronal loops, the magnetic field strength may be relatively constant. There was therefore the additional hope that thermal cyclotron lines might be detected as emission that is enhanced above the optically thin bremsstrahlung.

The active regions AR 3804 and AR 3828 were observed on July 19 and 28, 1982, respectively, with the entire VLA (B configuration) at 1380 MHz, 1540 MHz and 1705 MHz. The position of AR 3804 was N09 W64 at 1300 UT on July 19 and the position of AR 3828 was N06 E27 at 1300 UT on July 28. The active regions were successively observed for 10 minute periods at the three frequencies, and this was followed by successive 2 minute observations of the calibrator source OI 318. The enitre 36 minute sequence was repeated for an eight hour period centered on local noon. At these frequencies, the half-power beamwidth of the individual antennas is $\approx 31'$ and the synthesized beamwidth is $\approx 3'' \times 4''$. In

all cases the bandwidth was 12.5 MHz. The average correlated flux of 356 interferometer pairs was sampled every 10 s for both the left hand circularly polarized (LCP) and right hand circularly polarized (RCP) signals. The data were then calibrated according to the procedure described by Lang and Willson (1979) together with a correction for the difference in the signal from high temperature noise sources detected in each polarization channel. The assumed fluxes of the calibrator source OI 318 at 1380, 1540 and 1705 MHz were 1.73 Jy, 1.65 Jy and 1.6 Jy, respectively. At these frequencies the temperatures of the calibration noise sources are the same to within ± 5%. The calibrated data were then edited and used together with the standard CLEAN procedure to make the synthesis maps shown in Figures 3 and 4.

These maps show dramatic changes in the structure of the active regions at the three closely spaced frequencies. In Table I we give the brightness temperatures at several locations within the active regions where these temperature differences are particularly striking. The intensity within both the northern and southern components of AR 3804 (Fig. 3) varies by as much as a factor of 5 at some locations at the three frequencies. AR 3828 exhibits an enhancement in only one component of the active region (A, Fig. 4) where the brightness temperature at 1540 MHz is about a factor of 2.5 greater than at 1380 MHz and 1705 MHz. The V maps shown in Figure 4 indicate that the circularly polarized emission is also enhanced in the same part of the active region where the total intensity is the highest. We were unable to detect any polarized emission from AR 3804 to a limit of $< 10\%$.

These striking changes in source structure cannot be due to an artifact of the cleaning process, as they were also visible in the uncleaned, or "dirty" maps. If these changes were due to a systematic error in calibration

or to the confusion from neighboring sources located on the sun, then we would expect similar variations in all of the sources located within the antenna beam. For comparison, in Figure 5 we show synthesis maps of an active region located ≈ 3.2' west and ≈ 2.5' north of AR 3828 (AR 3828 NW) on July 28. These maps of total intensity indicate that the source structure and peak brightness temperature at the three frequencies are the same to within ≈ 15%.

3. DISCUSSION

The changes in source structure are difficult to explain by the conventional radiation mechanisms of gyroemission or thermal bremsstrahlung which predict gradual changes in brightness temperature and polarization over the observed frequency range. In the optically thick regime, the brightness temperature of a uniform source due to the bremssstrahlung and gyroemission vary as ν^{-2} and ν^{-1}, respectively, where ν is the observing frequency. Our observations however indicate much more rapid brightness temperature variations, with $T_b \propto \nu^{\pm 5}$ for some components (see Table I). These abrupt changes in brightness temperature can, however, be explained by cyclotron line emission.

The maximum brightness temperatures as a function of frequency of components A and B of AR 3804 and component A of AR 3828 NW have been plotted in Figure 6 with conservative error bars corresponding to the peak-to-peak fluctuations in the background noise temperature of the synthesis maps. We also show the brightness temperature of theoretical curves of cyclotron line emission for the harmonics s = 3, 4 and 5 and a number of different values of the magnetic field strenght, temperature, density, scale length and angle. We find that thermal cyclotron lines can explain the observed total intensity and

polarization of AR 3804 and AR 3828 with plausible physical parameters H = 125-180 G, an electron density $N_e = 3 \times 10^9$ cm^{-3}, an electron temperature $T_e = 1.5 \times 10^6$ K and a scale length $L = L_H = 1 \times 10^9$ cm. The observations of AR 3828 NW, can, however, be explained as either optically thick bremsstrahlung or gyroemission with $T_b = T_e = 1.4 \times 10^6$ K. The polarization data constrain the angle α to be $> 80°$ for AR 3804 and $\approx 20°$ for AR 3828. Under the assumption that the magnetic field projects radially outward from the surface of the sun into the corona, these angles are also plausible, as AR 3804 and AR 3828 were, respectively, near the solar limb and near central meridian, at the time of observation. These model curves are not unique, however, as the parameters can be adjusted to give acceptible agreement with the data.

There may also be alternative explanations of our data. One possibility is that the emission at each frequency originates at a different height above the active region where the physical conditions are also different. Observations at successively lower frequencies refer to successively higher levels in the solar atmosphere where the electron temperature and density and magnetic field systematically increase and decrease, respectively. The brightness temperature of optically thick emission ($T_b = T_e$) can therefore only decrease with increasing frequency, whereas the brightness temperature of optically thin emission ($T_b \approx T_e\tau$) may increase with increasing frequency. In Figure 6 we show power law fits to the brightness temperatures of components A and B of AR 3804. For component A, $T_b \propto \nu^{-4.1}$ so that the decrease in brightness temperatures might be attributed to an optically thick source in which the temperature systematically decreases with decreasing height. For component B, $T_b \propto \nu^{+7.7}$, suggesting an optically thin source in

which the temperature or the density or both change with height. This alternative explanation however, cannot explain the observations of AR 3828 which show neither a systematic increase or decrease of the brightness temperature with frequency. Because thermal cyclotron lines can explain the observed data with plausible physical parameters while conventional radiation mechanisms cannot, we believe that we have a possible detection of cyclotron lines. This has important implications for the combined measurements of bremsstrahlung and cyclotron lines provide a sensitive probe of the physical properties of coronal loops. For instance, it is known that the electron temperature of quiescent coronal loops have a narrow range of temperature between 1 and 3 x 10^6 K. A measurement of the electron temperature, say using the Solar Maximum Mission X-ray instruments (when it is repaired in 1984) combined with VLA observations of the radio brightness temperature and bremsstrahlung optical depth will give a reliable measurement of the emission measure. As illustrated in Figures 1, 2 and 6, the central frequencies of the cyclotron lines provide a sensitive measurement of the magnetic field strength, for a change of only 20 Gauss produces a 170 MHz shift in the central frequency of the line. Carefully calibrated, high resolution maps of the total intensity and circular polarization of active regions at uniformly spaced frequencies over a frequency range of ≈ 1 GHz may provide a detailed description of the magnetic field, temperature and density of the active region. Measurements of these effects can probably best be made with the VLA which provides sufficient angular resolution to resolve the different sources of cyclotron lines. The poorer angular resolution of single antennas would combine the signals from different sources, and the cyclotron lines might be lost in the superposition of the different sources which radiate at different frequencies.

ACKNOWLEDGEMENTS

The author wishes to thank Kenneth R. Lang for helpful discussions. Radio interferometric studies at Tufts University are supported under grant AFOSR-83-0019 with the Air Force Office of Scientific Research. The VLA is operated by Associated Universities, Inc., under contract with the National Science Foundation.

REFERENCES

Alissandrakis, C.E., Kundu, M.R. and Lantos, P.:1980, Astron. Astrophys. 82, 30.

Enome, S., Kakinuma, T. and Tanaka, H.:1969, Solar Phys. 6, 428.

Gel'freikh, G.B. and Lubyshev, B.I.:1979, Sov. Astron. A.J. 23, 316.

Ginzburg, V.L. and Zheleznyakov, V.V.:1959, Sov. Astr. A.J. 3, 235.

Kakinuma, T. and Swarup, G.:1962, Astrophys. J. 136, 975.

Kaverin, N.S., Kobrin, M.M., Kovshunov, A.I. and Sushunov, V.V.:1980, Sov. Astron. A.J. 24, 442.

Kundu, M.R.:1959, Ann. d'Ap. 22, 1.

Kundu, M.R. and Velusamy, T.:1980, Astrophys. J. Lett. 240, L63.

Kundu, M.R., Schmahl, E.J. and Rao, A.P.:1981, Astron. Astrophys. 94, 72.

Kuznetsov, V.D. and Syrovatskii, S.I.:1981, Solar Phys. 69, 361.

Lang, K.R.:1974, Solar Phys. 36, 351.

Lang, K.R. and Willson, R.F.:1979, Nature 278, 24.

Lang, K.R. and Willson, R.F.:1982, Astrophys. J. Lett. 255, L111.

Lang, K.R., Willson, R.F. and Rayrole, J.:1982, Astrophys. J. 258, 384.

Lang, K.R., Willson, R.F. and Gaizauskas, V.:1983, Astrophys. J. 267, 455.

Pallavicini, R., Sakurai, T. and Vaiana, G.S.:1981, Astron. Astrophys. 98, 316.

Stepanov, K.N.:1959, Sov. Phys. JETP. 8, 195.

Syrovatskii, S.I. and Kuznetsov, V.D.:1980, in M.R. Kundu and T.E. Gergeley (eds.), 'Radio Physics of the Sun', IAU Symp. 86, 109.

Zheleznyakov, V.V.:1970, in 'Radio Physics of the Sun and Planets', New York, Pergamon Press.

Zheleznyakov, V.V.:1962, Sov. Astr. A.J. 6, 3.

Zheleznyakov, V.V. and Zlotnik, E. Ya.:1980, Solar Phys. 68, 317.

Zheleznyakov, V.V. and Zlotnik, E. Ya.:1980, Sov. Astron. A.J. 24, 448.

Zheleznyakov, V.V. and Tikhomorov, Yu. V.:1982, Solar Phys. 81, 121.

TABLE I. Maximum brightness temperatures, T_b(max), of components within AR 3804, AR 3828 and AR 3828 NW at different frequencies.

	Component	1380 MHz T_b (°K)	1540 MHz (°K)	1705 MHz (°K)
AR 3804	A	1.3×10^6	4.6×10^5	5.3×10^5
	B	3.1×10^5	4.7×10^5	1.5×10^6
AR 3828	A	6.2×10^5	1.5×10^6	6.5×10^5
	B	1.9×10^6	1.9×10^6	2.1×10^6
AR 3828 NW	A	1.2×10^6	1.4×10^6	1.4×10^6

FIGURE LEGENDS

Figure 1. Theoretical plots of the brightness temperature, T_B, and degree of circular polarization, ρ_c, of thermal cyclotron lines at different harmonics S = 2, 3, 4 and 5 for magnetic field strengths H = 120, 140, 160 and 180 G, and angles, α, of 10°, 30°, 60° and 80°. These curves were generated using an electron temperature $T_e = 2 \times 10^6$ K, an electron density $N_e = 5 \times 10^9$ cm^{-3} and a path length $L = L_H = 1 \times 10^9$ cm.

Figure 2. Theoretical plots of the brightness temperature, T_B, and degree of circular polarization, ρ_c, of thermal cyclotron lines at different harmonics S = 3, 4, and 5 for magnetic field strengths H = 300, 400, 500 and 600 G, and angles, α, of 10°, 30°, 60° and 80°. These curves were generated using an electron temperature $T_e = 2 \times 10^6$ K, an electron density $N_e = 5 \times 10^9$ cm^{-3} and a path length $L = L_H = 1 \times 10^9$ cm.

Figure 3. VLA synthesis maps of the total intensity, I, of AR 3804 at three closely spaced frequencies using data obtained during an eight hour period on July 19, 1982. The synthesized beamwidth is $\theta \approx 3'' \times 4''$. The contours of the map mark levels of equal brightness temperature. The outermost contour and the contour level are equal to 3.2×10^5 and 1.6×10^5 K, respectively. The positions of components A and B, referred to in the text and Table I, are marked with a cross. The angular scale can be determined from the 60" spacing between the fiducial marks on the axes.

Figure 4. VLA synthesis maps of the total intensity, I (top), and circular polarization, V (bottom) of AR 3828 at three closely spaced frequencies using data obtained during an eight our period on Juley 28, 1982. The synthesized beamwidth is $\theta \approx 3'' \times 4''$. The contours of the maps mark levels of equal brightness temperature, and the solid and dashed contours of the V maps denote positive and negative values of V, respectively. The outermost contour and the contour level of the I maps are equal to 4.3×10^5 and 2.2×10^5 K, respectively. The contours of the V maps are drawn at -3.6×10^5, -3.2×10^5, $-2.8 \times 10^5 \ldots 2.1 \times 10^5$ K. The positions of components A and B, referred to in the text and Table I, are marked with a cross. The maximum degree of circular polarization, ρ_c, is $\approx 35\%$ at each of the three frequencies in component A. The angular scale can be determined from the 30" spacing between the fiducial marks on the axes.

Figure 5. VLA synthesis maps of the total intensity, I, of an active region, AR 3828 NW, located $\approx 5'$ northwest of AR 3828 on July 28, 1982. The contours of the maps mark levels of equal brightness temperature, where the outermost contour and the contour interval are equal to 2.9×10^5 and 1.4×10^5 K, respectively. The position of maximum intensity is marked with a cross. The angular scale can be determined from the 30" spacing between the fiducial marks on the axes.

Figure 6. Theoretical plots of the brightness temperature of thermal cyclotron lines at different harmonics S = 2, 3, 4 and 5 for magnetic field strengths of H = 125, 150 and 180 G. The maximum brightness temperatures observed for components A and B of AR 3804 and components A of AR 3828 and AR 3828 NW are also plotted with error bars corresponding to the peak-to-peak fluctuations in the background temperature of the synthesis maps. The theoretical curves for AR 3804 were calculated assuming an electron temperature of $T_e = 1.5 \times 10^6$ K, an electron density, $N_e = 3 \times 10^9$ cm^{-3}, a path length $L = L_H = 1 \times 10^9$ cm, and an angle, $\alpha = 80°$. The curves for AR 3828 were calculated with the same values of electron density and path length but with $T_e = 1.8 \times 10^6$ K, and $\alpha = 20°$. The dashed lines refer to power-law fits to the observed brightness temperatures. The data for AR 3828 are fit by optically thick thermal bremsstrahlung with $T_b = T_e = 1.4 \times 10^6$ K.

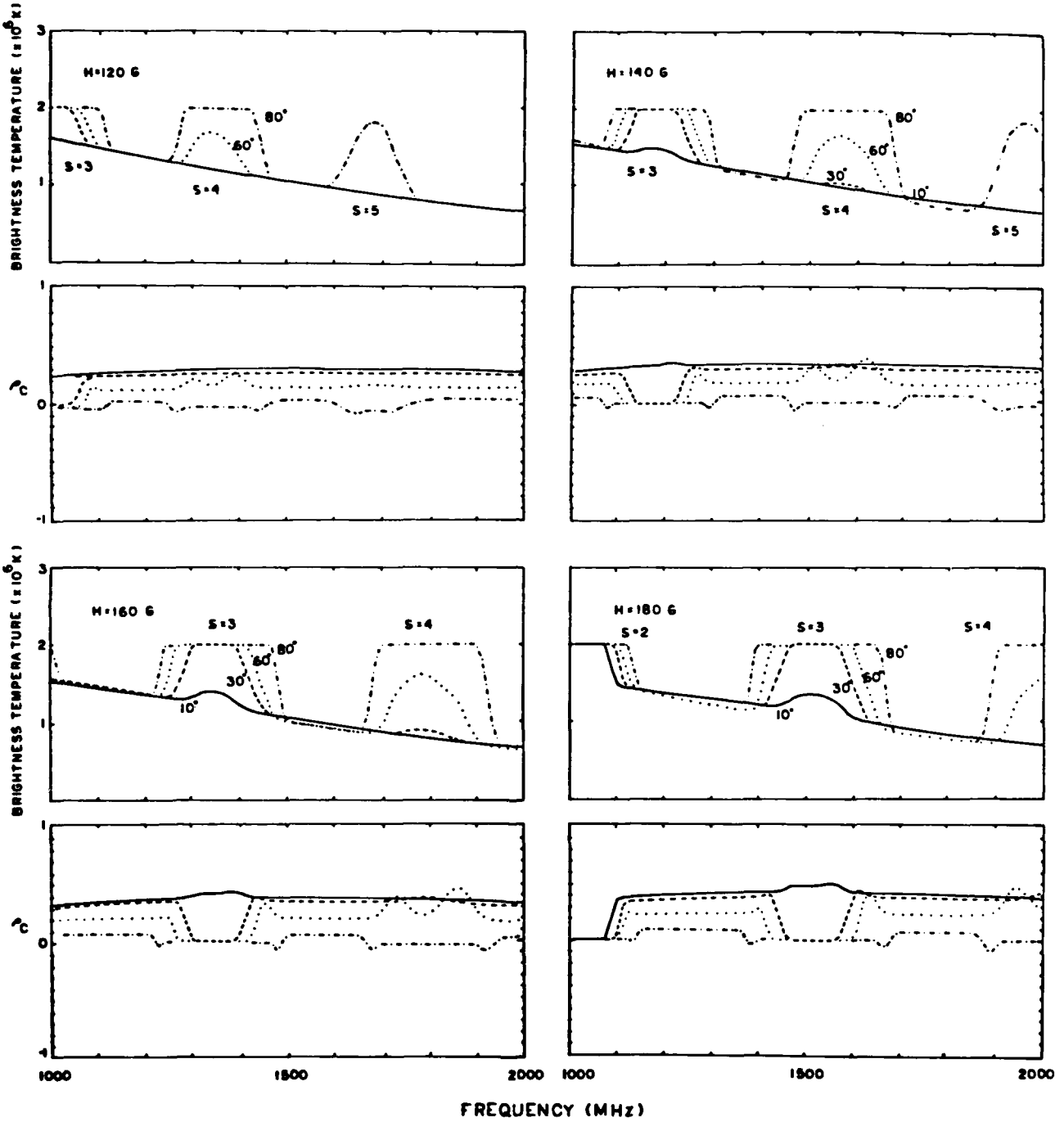
BRIGHTNESS TEMPERATURE (x10^6 K)
H=120 G
S=3
S=4
S=5
80°
60°
H=140 G
S=3
S=4
S=5
80°
60°
30°
10°
ρc
H=160 G
S=3
S=4
80°
60°
30°
10°
H=180 G
S=2
S=3
S=4
80°
60°
30°
10°
1000
1500
2000
FREQUENCY (MHz)

Fig 1.

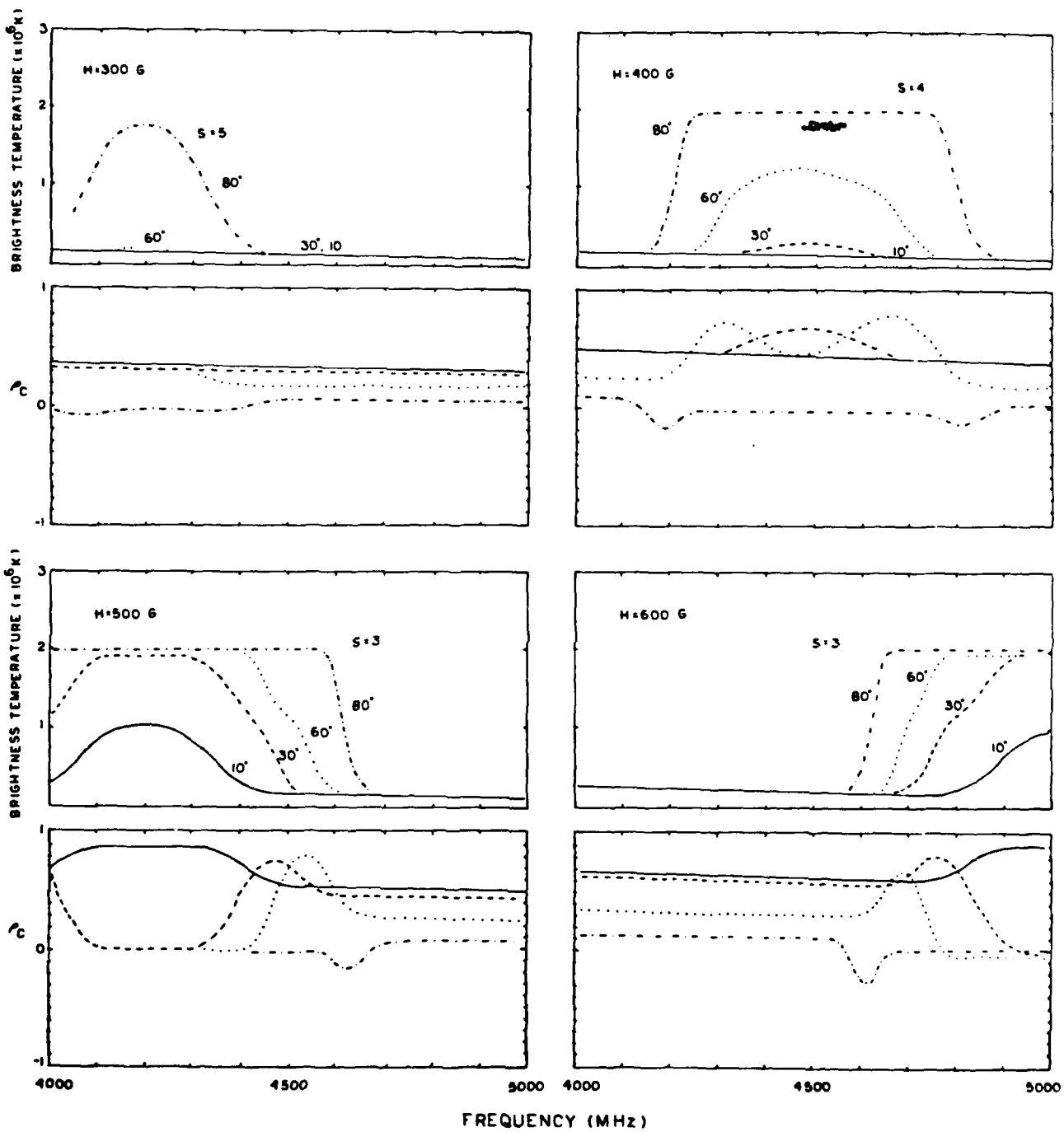
BRIGHTNESS TEMPERATURE (x10⁶K)
H=300 G
S=5
80°
60°
30°, 10
H=400 G
S=4
80°
60°
30°
10°
ρc
H=500 G
S=3
80°
60°
30°
10°
H=600 G
S=3
80°
60°
30°
10°
4000
4500
5000
FREQUENCY (MHz)

Fig. 2

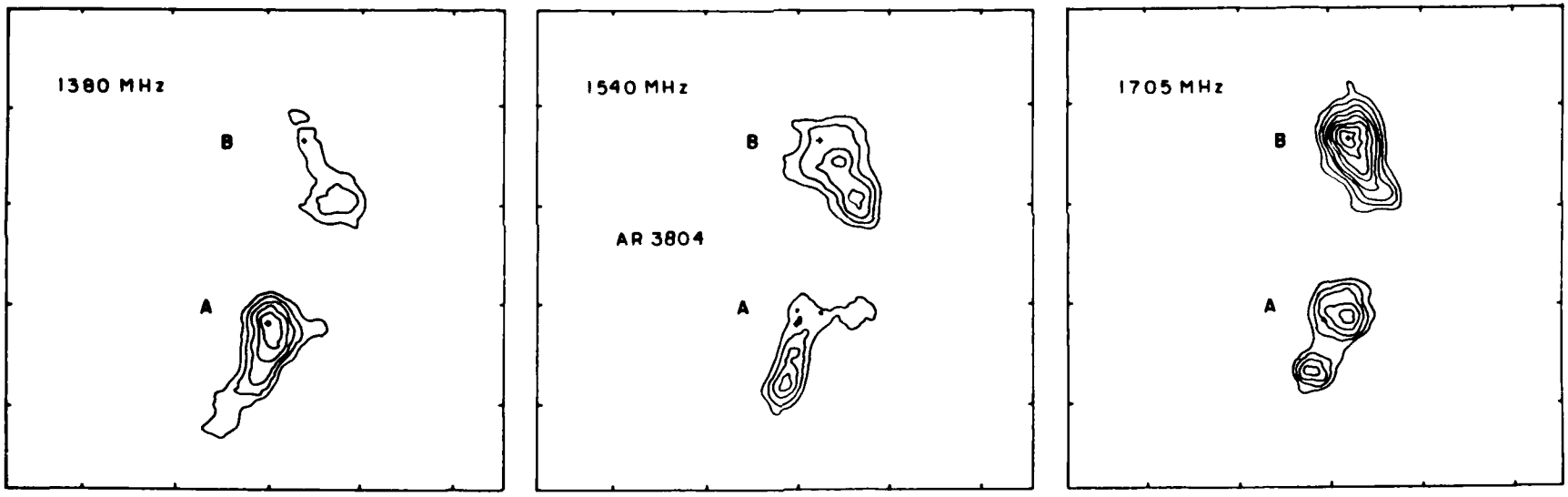
1380 MHz
B
A
1540 MHz
B
AR 3804
A
1705 MHz
B
A

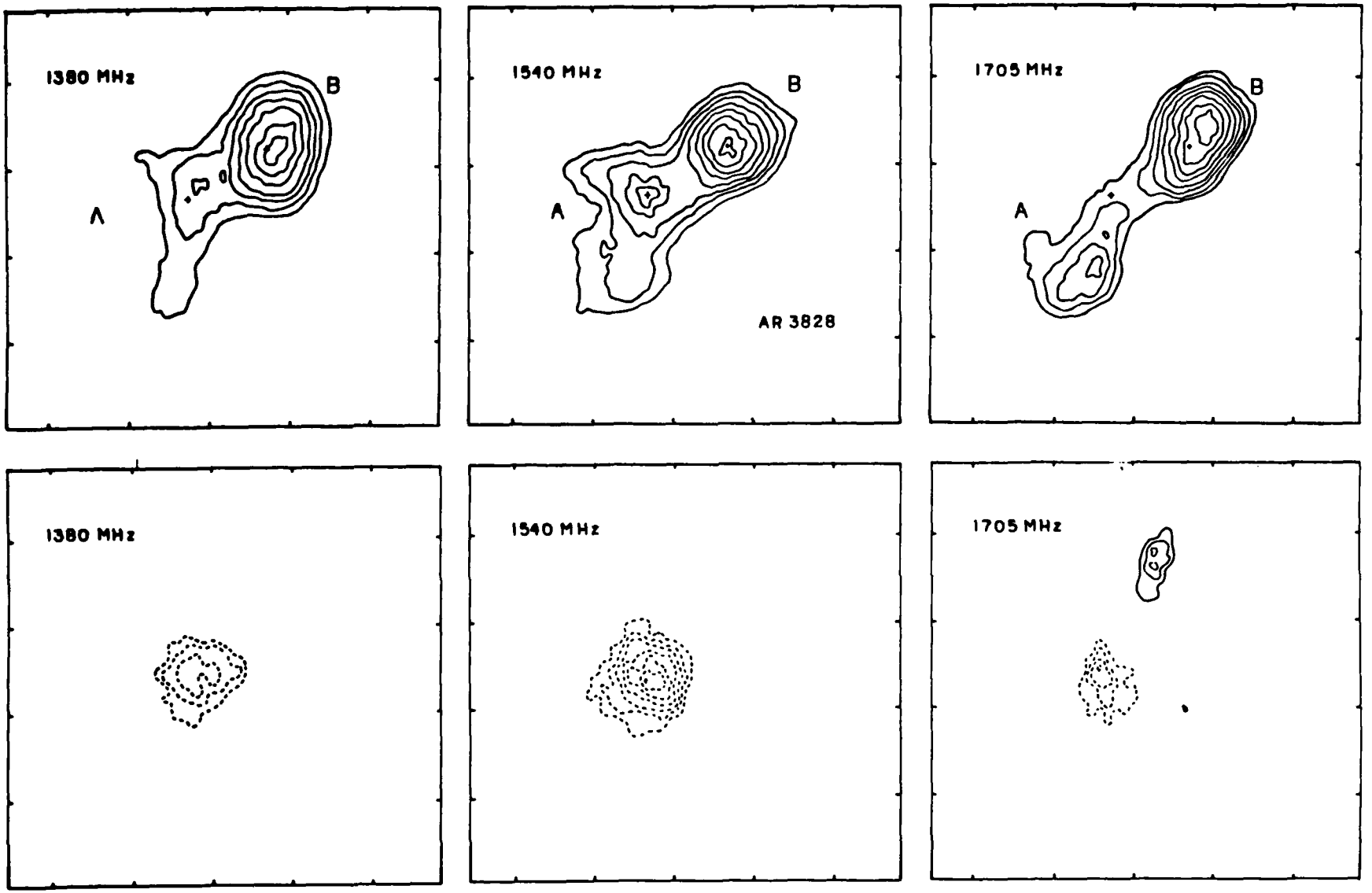
1380 MHz
A
B
1540 MHz
A
B
AR 3828
1705 MHz
A
B
1380 MHz
1540 MHz
1705 MHz

Fig. 4

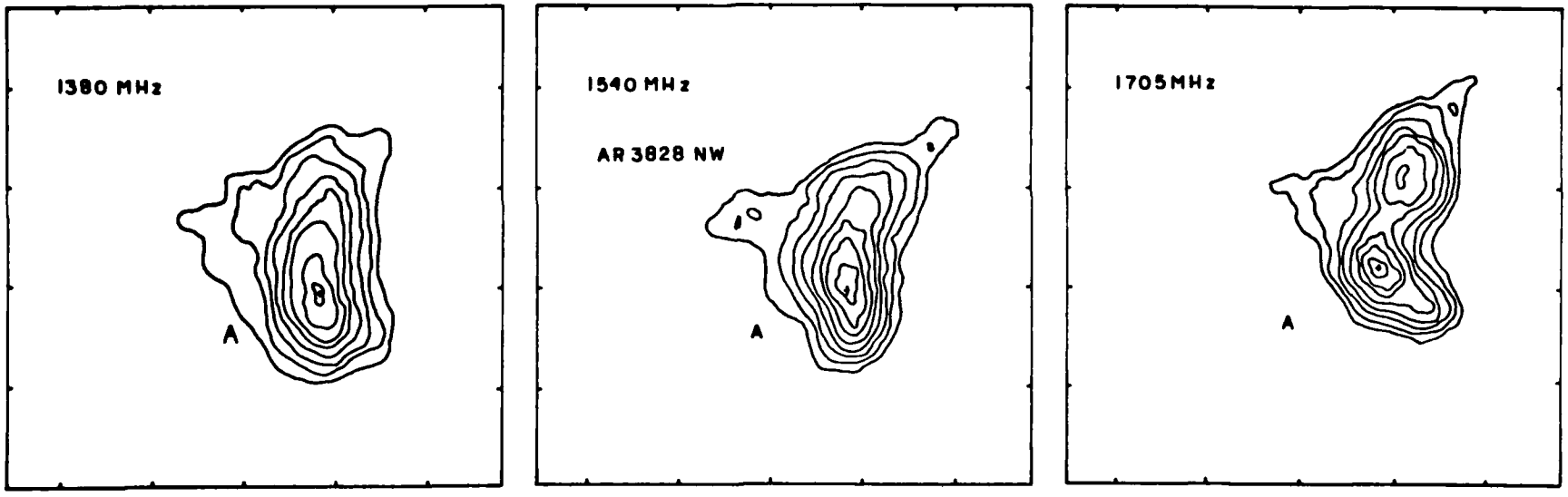

Fig. 5

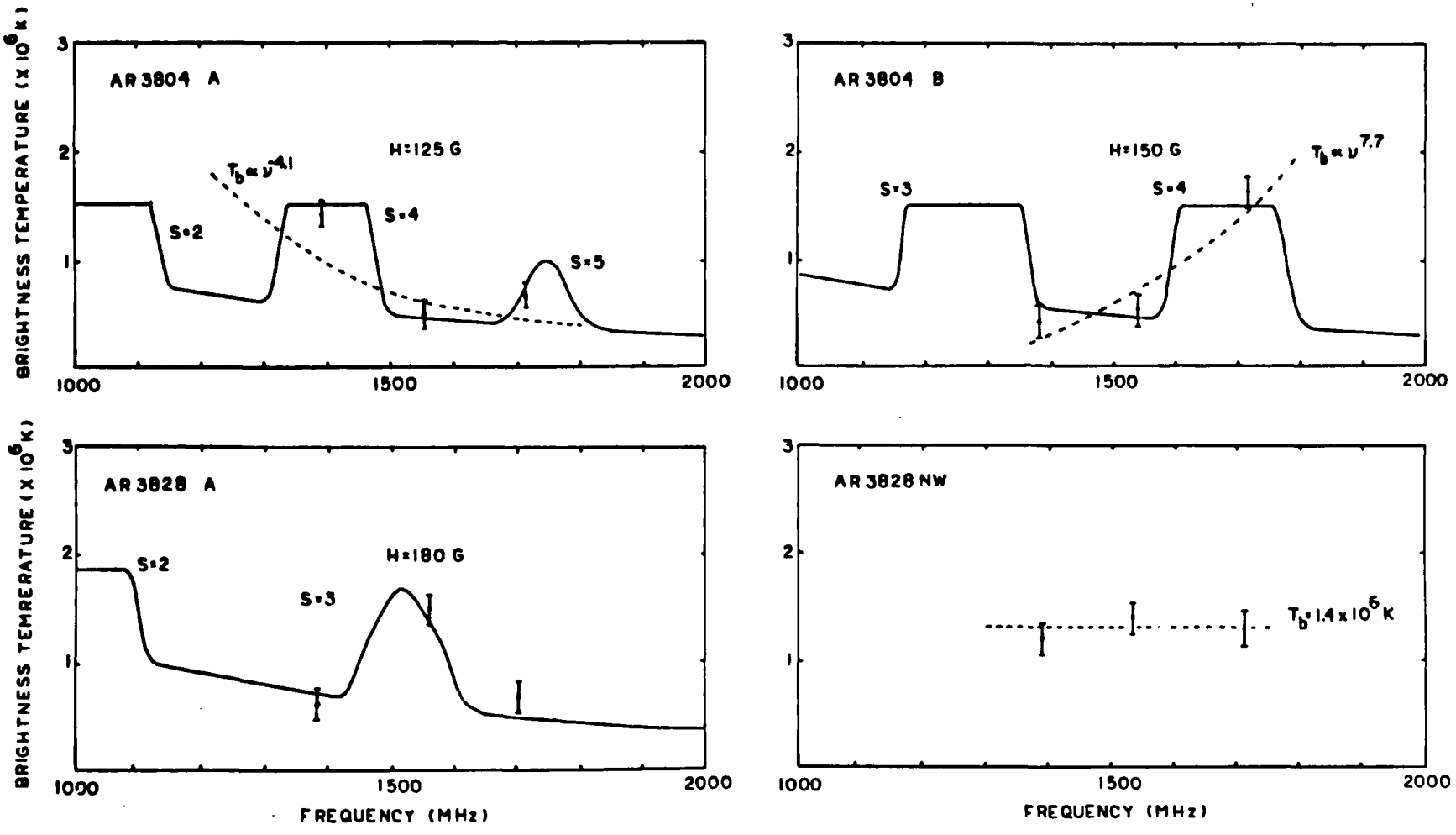
AR 3804 A
H=125 G
$T_b \propto \nu^{-4.1}$
S=2
S=4
S=5
AR 3804 B
H=150 G
$T_b \propto \nu^{7.7}$
S=3
S=4
AR 3828 A
H=180 G
S=2
S=3
AR 3828 NW
$T_b = 1.4 \times 10^6$ K
BRIGHTNESS TEMPERATURE ($\times 10^6$ K)
BRIGHTNESS TEMRERATURE ($\times 10^6$ K)
FREQUENCY (MHz)
FREQUENCY (MHz)
1000
1500
2000
1
2
3

Fig. 6

END

DATE
FILMED

1-84

DTIC